

Explaining Human Preferences via Metrics for Structured 3D Reconstruction

Jack Langerman
Independent Researcher *
jack@jackml.com

Yuzhong Huang
HOVER Inc.
yuzhong.huang@hover.to

Denys Rozumnyi
ETH Zurich / Czech Technical University in Prague
rozumden@gmail.com

Dmytro Mishkin
HOVER Inc. / Czech Technical University in Prague
dmytro.mishkin@hover.to

Abstract

“What cannot be measured cannot be improved” while likely never uttered by Lord Kelvin, summarizes effectively the purpose of this work. This paper presents a detailed evaluation of automated metrics for evaluating structured 3D reconstructions. Pitfalls of each metric are discussed, and a thorough analysis through the lens of expert 3D modelers’ preferences is presented. A set of systematic “unit tests” are proposed to empirically verify desirable properties, and context aware recommendations as to which metric to use depending on application are provided. Finally, a learned metric distilled from human expert judgments is proposed and analyzed.

1. Introduction

Benchmarks have been key drivers of progress in computer vision, the canonical example is certainly ImageNet [31], but prominent examples abound beyond image classification: object tracking [21, 23], image retrieval [4, 30], image matching [20], 6D pose estimation [15], optical flow [27], etc. Benchmarks have two main components – the dataset and the metrics. While the data is the single most important component, the progress is hard without being able to answer the question, “progress on what?” Good metrics are the quantitative answer to this question. While metrics do not need to be perfect, their gradient should point the progress in the right direction.

We consider an area of structured and semi-structured reconstruction and recognition, which gained some popularity recently [1] [19] [5]. Given a set or sequence of sensory data, such as ground images [22], satellite images [9], or aerial LiDAR [33], the goal is to produce a wireframe or a CAD model of the building or other structures. Natu-

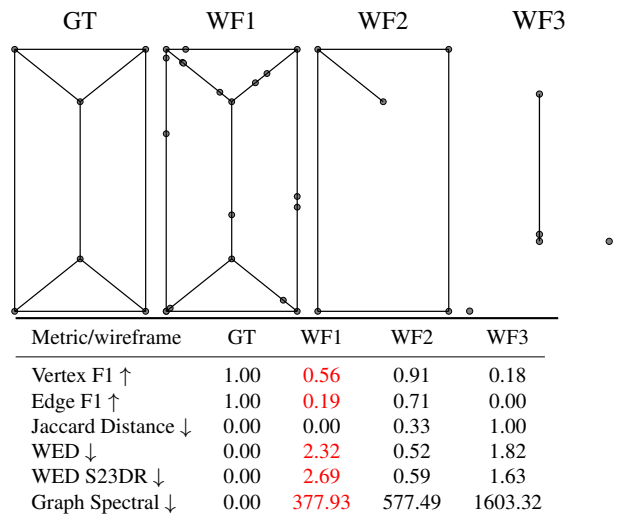


Figure 1. Motivational example for this work. While humans tend to sort the wireframes from best to worst in the presented order, popular metrics sort them differently, sometimes completely inverting the order. Top row, left to right: ground truth wireframe, wireframe with edges split into several segments, maintaining geometrical and topological accuracy, wireframe with missing vertices and edges, wireframe with only one correct vertex. Bottom row: distances between GT and respective wireframe. Numbers that change sorting are in red.

rally, the modeling output is presented as a graph with vertices (such as house apex point, etc.) and edges (roof line, etc.). Several datasets have been recently proposed [22, 33] for the task. The issue, however, is that hardly a pair of publications in the area use the same metric to evaluate quantitative results. Some of them use recognition metrics such as precision and recall on vertices and edges [25] or a more enhanced version such as Structured Average Precision [26, 36]. Others opt for graph-based metrics, such as the Wireframe Edit Distance (WED) [8, 24, 25]. Finally, some methods treat the problem similarly to the point

¹Now at Apple

cloud registration problem and report Chamfer Distance (CD) [10, 16, 17]. Other related fields, like structure from motion, use downstream metrics, such as image generation quality [6] and camera pose accuracy [20]. The difficulty here is related to the fact that structured reconstructions often have different goals. For instance, one purpose of the reconstructed wireframes is to represent building floorplans and answer questions such as "what is the area of the bedroom?" Within this formulation, a black-box model, *e.g.* visual-and-language model (VLM), which takes an image as an input and outputs a correct estimate, would be a perfect match. On the other hand, a floorplan or a blueprint has value for record-keeping, planning, and other applications that cannot be easily replaced with a black-box model.

Finally, many existing metrics, while useful, often fail to deliver value in practice when comparing two imperfect estimations, and designing metrics that effectively compare a pair of "very good" and a pair of "very bad" solutions at the same time is also non-trivial.

Moreover, there is evidence [22] that some metrics can be "hacked" or exploited in such a way that obviously bad solutions have better scores than flawed but ultimately quite reasonable solutions. Such examples include a number of corner cases, which can cause existing metrics to become useless in practical scenarios. For instance, in the case where long edges are split into smaller, yet perfectly collinear, pieces, *e.g.* Fig. 1, most commonly used metrics, such as edge F1, vertex F1, and Wireframe Edit Distance, fail completely and prefer much worse solutions.

This paper makes the following contributions:

- (1) Measure the perceived quality of reconstructions by human domain experts, and infer a global ranking of all structured reconstructions. This ranking is then compared to the ranking given by all metrics.
- (2) Show how well existing metrics agree with human preferences and how much they correlate with each other.
- (3) Propose a set of "unit-tests" for testing the properties of the metrics.
- (4) Introduce a simple learned metric, which correlates well with human judgment.
- (5) Make recommendations of which metrics to use depending on the use case.

2. What do we actually need from the wireframe comparison metrics?

We consider semi-automated 3D modeling as a target task with enough generality to drive progress that can smoothly scale to fully-automated modeling, but is still tractable and reliable for commercial applications today.

For this task, the wireframe representation is estimated from some "raw" inputs such as images or a LiDAR point cloud and then transferred to the human experts to (1) ap-

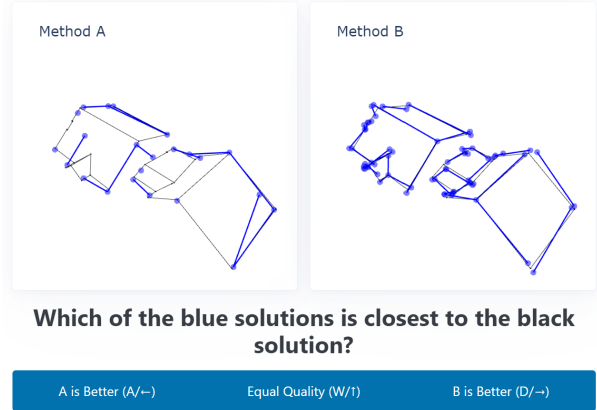


Figure 2. Wireframe ranking interface for human annotators.

prove it, (2) correct it and then approve, (3) reject and create the model from scratch manually.

We argue that such task formulation creates an implicit usefulness ranking over reconstructions (and thereby over reconstruction methods). Otherwise, without considering human involvement, everything becomes binary – either the model is good enough to be used (*e.g.* for 3D printing, measurement extraction), or it is not.

For this reason, we consider the following experimental setup to benchmark the wireframe comparison metrics. A pool of professional 3D modelers, whose everyday job is to create CAD-like models from raw data such as images, is asked to rank pairs of wireframes. An example of the ranking setup is shown in Fig. 2. All wireframes are superimposed with ground truth models, and the annotators can translate, scale, and rotate the wireframes in 3D.

The wireframes are drawn from two pools, as described below. We then evaluate how the existing metrics agree with the judgment of professional human 3D modeling experts.

Pool1– S^23DR . We acquire a representative set of S^23DR challenge entries [22] and PC2WF [24] baseline. These wireframes were algorithmically (and with the help of deep-learned models) reconstructed from multiview inputs with the goal of minimizing a variant of WED. We include top-10 entries, and the team names are used as identifiers. The ground truth models were created by human experts and have undergone significant validation. The input data were captured by users on mobile phones in North America.

Pool2 — Corrupted ground truth. We apply one of the following operations on the ground-truth wireframes from Pool 1 – examples are shown in Fig. 3:

- (deform_{low, medium, high}) Split the edge into several edges and perturb the vertices positions, without breaking the topology.
- (perturb_{low, medium, high}) Split the vertex into several ones. Each of the new vertices is randomly shifted from the ground truth. If the original vertex was con-

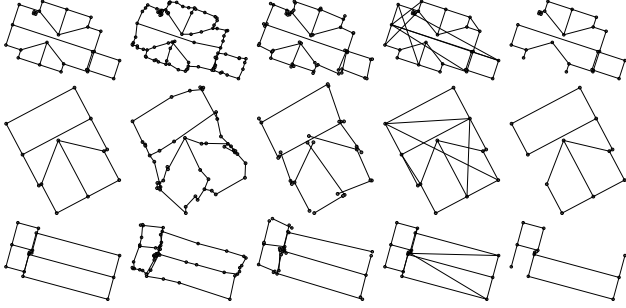


Figure 3. Examples of corrupted ground truth wireframes, used for wireframe ranking. Left to right: ground truth, deformed edges (deform_medium), vertex duplication and random movement (perturb_medium), edge addition (add_low), edge deletion(remove_low).

nected to multiple neighbors, randomly decide which of the new vertices is connected to which neighbors.

- (add_{low, medium, high}) Randomly add wrong edges to the model.
- (remove_{low, medium, high}) Randomly delete some of the vertices and all the edges connected to them.

Unit-tests. In addition to being aligned with human judgment, we also propose a set of "unit-tests" for the metrics, which we believe are reasonable, and check if the metrics satisfy these requirements. For example, if wrong edges E_1 and E_2 are added to the GT model, the metric should score the resulting wireframe lower than if E_1 or E_2 are added separately.

Desired properties of dissimilarity scores. The following are the formal properties of mathematical metrics, as well as additional properties relevant to evaluating dissimilarity in structured reconstruction tasks.

Identity of Indiscernibles: This property ensures that identical inputs receive a dissimilarity score of zero, indicating perfect similarity. For any reconstruction x , a metric d satisfies this property if $d(x, x) = 0$.

Symmetry: A symmetric metric produces the same dissimilarity score regardless of the order of the inputs. For reconstructions x and y , the metric satisfies symmetry if $d(x, y) = d(y, x)$.

Triangle Inequality: The triangle inequality ensures that for any three reconstructions x , y , and z , the dissimilarity between x and z is less than or equal to the sum of dissimilarities between x and y , and y and z . This relationship is expressed as $d(x, z) \leq d(x, y) + d(y, z)$.

Monotonicity: This property describes how the dissimilarity score behaves when components (such as vertices or edges) are removed from a reconstruction. A metric satisfies monotonicity if the dissimilarity score does not increase when wrong vertices or edges are deleted. Similarly, the dissimilarity must not increase when correct vertices or

edges are added.

Smoothness: This property holds when the metric changes smoothly over time (either increases or decreases). This is evaluated by moving random vertices with small increments and checking the variance of the differences in the score. We use the following perturbations to simulate better or worse reconstructions: (i) remove correct edges from the ground truth wireframe; (ii) add wrong edges to the ground truth wireframe; (iii) disconnect ground truth edges; (iv) remove correct vertices; (v) move ground truth vertices to the wrong location. For every perturbation, we apply it 10 times and declare an example monotonic if it is strictly increasing (or decreasing as appropriate) for those continuous 10 perturbations.

3. Metrics

The following metrics are considered:

WED – Wireframe Edit Distance was proposed by Liu *et al.* [24] as an extension of the Graph Edit Distance (GED) [32]. GED quantifies the distance between two graphs as the minimum number of elementary operations (inserting and deleting edges and vertices) required to transform one graph into another. WED extends this to wireframes (graphs with node positions and edge lengths) and proposes a cheap approximation to the NP-Hard problem of computing the optimal sequence of edits. Concretely, an assignment is first computed between the predicted and ground-truth vertices, and a cost is paid proportional to the distance between matched vertices. Next, unmatched vertices are deleted, and missing vertices are inserted (paying a cost proportional to the number of inserted/deleted vertices). Finally, given the vertex assignments, missing edges are inserted and extra edges deleted, paying a cost proportional to their length. In order to use WED, one needs to decide on the cost of insertion and deletion of the vertices, as well as the order of operations, and method of computing vertex/edge assignment. WED was used to determine the winner in Building3D [33] and S^23DR [22] CVPR Challenges.

ECD – Edge Chamfer Distance. ECD is commonly used in structured reconstruction papers [10, 16, 17]. We consider a family of chamfer-like metrics between two sets A and B . The general form is:

$$d(A, B) := \inf_{\pi_{AB}: A \rightarrow B} \mathbb{E}_{a \in A} [f(a, \pi_{AB}(a))] , \quad (1)$$

where π_{AB} represents an assignment from elements in A to elements in B , and f is typically an ℓ_p norm. Different constraints on π_{AB} yield different metrics:

- The classical chamfer distance corresponds to choosing $\pi_{AB}(a) = \arg \min_{b \in B} f(a, b)$, *i.e.* nearest neighbor matching.

- The most constrained version requires π_{AB} to be a bijective matching, which can be computed via the Hungarian algorithm and is equivalent to the Earth Mover’s Distance when f is the ℓ_p norm.

Length Weighed Spectral Graph Distance – SD incorporate both topological and geometric information by framing graph (wireframe) distance in terms of distances between the spectra of weighted graph Laplacians. We measure the spectral distance using the 2-Wasserstein metric between the eigenvalue distributions:

$$SD(G_1, G_2) := W_2(\lambda(L_1), \lambda(L_2)), \quad (2)$$

where $\lambda(L)$ denotes the spectrum of the Laplacian L . For a graph $G = (V, E)$, the weighted graph Laplacian is defined:

$$L := D - A \quad (3)$$

where D is the weighted degree matrix ($|V| \times |V|$ diagonal matrix with each diagonal entry containing the sum of the lengths of edges incident to that vertex), and A is the weighted adjacency matrix ($|V| \times |V|$ with $A_{ij} = \|V_i - V_j\|_2$ if $(i, j) \in E$ and 0 otherwise).

Corner and Edge Metrics. We also compute precision, recall, and F1 scores for both corners and edges. For corners, we consider a prediction correct if it lies within a distance threshold of a ground truth corner. For edges, we use the Hausdorff distance between line segments to determine matches. These metrics provide an intuitive measure of the topological accuracy of the predicted wireframes.

Hausdorff Distance measures the maximum of minimal distances between two sets of points. For wireframes, we sample points along the edges and compute the Hausdorff distance between these point sets, providing a measure of geometric similarity that considers both corner positions and edge geometry.

Intersection over Union is a popular metric in a wide range of fields, *e.g.* segmentation, tracking, object detection. However, it is rarely used to assess the quality of wireframe reconstructions. We extend the definition of the wireframe as a set of cylinders with a fixed radius (the only hyperparameter of this metric) and define the metric as an IoU between two sets of cylinders, given by two wireframe reconstructions that need to be compared. The point sampling approximation is considered: sample random points from both sets of cylinders and compute the average number of times when the point falls inside of both sets of cylinders. The **Jaccard distance** is reported between two sets.

Visual-and-language models could potentially be used for this task. We consider 4o, o1 [13], Grok 2 [34], qwen-2.5 [18], pixtral 12b [2], claude 3.5 and 3.7 [3], gemini 2.0 and gemini 2.0-flash [12], and models via OpenRouter [28]. The prompts are provided in the supplementary.

Learned metric. We also explore how to transfer our annotations directly into a metric. For that, we propose to learn a metric with transfer learning. First, reconstruction and ground-truth wireframes are plotted in 3D and rendered from a canonical viewpoint. Then, we extract DiNOv2 [29] features on those renderings. An MLP-based regression head is then trained to score those renderings based on the extracted features. Assuming Bradley–Terry [7] probability model, we use annotations to supervise the training. Cross-entropy loss is minimized with a batch size of 16 to train the scoring head. We use 10-fold cross validation splitting the data such that the sets of ground truth structures and reconstruction methods used in train and test are disjoint. We observe average accuracy across the folds of 76%

4. Experiments

Human wireframe ranking and its consistency. To determine which of the metrics under consideration are most appropriate, we employ three groups of people to provide pseudo-ground-truth rankings of the solutions. The first and biggest group is made up of human 3D modeling experts who professionally create CAD models of objects from photos. The second group is computer vision researchers, and finally, the third group is people who do not work with 3D modeling in their daily lives. There are 11, 4, and 3 people in those groups respectively.

Annotators were shown pairs of reconstructions of the same structure, and asked to specify which reconstruction most closely matched the superimposed corresponding gold-standard wireframe. An example of the user interface is shown in Fig. 2. Annotators were able to zoom, pan, and rotate, allowing them to examine the solutions from all sides if needed; the viewpoint of both solutions is synchronized to ease the comparison. Most annotators rated around 3500 pairs.

Rater Reliability. We quantify rater reliability using two complementary methods: self-consistency and correctness on synthetic samples.

Correctness on Synthetic Samples. We introduced synthetic pairs of wireframes with known ground-truth rankings based on systematically applied ”corruptions.” Each corruption type featured ”Low,” ”Medium,” and ”High” severity levels. We treat the ”low” vs ”high” per each corruption type to be obvious enough that if annotators rank them differently, it can be treated as a labeling error, *e.g.* because of wrong clicks. Average rater accuracy on these ”easy” pairs is 98.3%.

Self-Consistency. We assessed intra-rater reliability by measuring how consistently annotators rated repeated pairs of wireframes, occasionally reversing pair order to mitigate order biases. These repeated evaluations constituted only a small subset of the total ratings. The average self-

Annotation agreement

	A	B	C	D	E	F	G	H	I	J	K	Des0	Des1	Des2	CV0	CV1	CV2	CV3	learned_metric_xval	corner_f1	corner_offset	edge_dist	edge_chamfer_bi	spectral_optimal_l1	WED_mnn	WED_ap	WED_prereg	random	claude-3.5	claude-3.7	claude-3.7-thinking	gemini-2.0-flash-001	gemini-2.0-flash-lite-001	gpt-4o-2024-11-20	gpt-4o	grok-2-vision-1212	qwq2.5-v1.7b-instruct	pixtral-12b	backpack		
A	100	81	79	86	88	87	74	72	70	72	73	75	84	84	85	87	88	78	82	82	78	79	72	77	77	73	73	67	67	50	50	54	52	50	47	52	52	50	54	50	53
B	81	100	81	83	82	81	73	71	70	69	67	72	82	80	85	82	83	79	77	83	78	80	71	74	71	67	74	65	70	51	50	42	42	54	63	67	67	54	63	45	58
C	79	81	100	81	84	81	73	67	68	68	72	73	77	77	81	84	80	75	77	77	73	74	68	77	74	65	71	63	67	51	27	41	66	40	31	68	68	68	68	40	40
D	86	83	81	100	86	85	78	74	73	73	77	79	85	85	85	85	87	83	82	84	81	78	75	77	76	73	72	64	70	51	39	51	55	52	47	58	63	63	64	55	48
E	88	82	84	86	100	89	76	71	72	72	75	77	86	88	88	92	89	81	83	83	77	78	71	80	77	73	74	66	67	50	43	42	52	45	45	55	62	63	60	50	46
F	87	81	81	85	89	100	75	70	71	72	74	76	87	87	87	90	87	79	82	82	76	77	71	79	77	71	73	66	67	50	40	50	48	51	47	58	59	58	64	50	46
G	74	73	72	78	76	75	100	83	87	83	85	81	82	78	78	76	80	86	80	80	85	70	83	71	68	64	68	63	67	56	36	45	56	42	48	58	62	62	67	50	47
H	72	71	67	74	71	70	83	100	79	81	78	75	76	70	73	69	72	79	74	81	88	70	90	65	61	61	69	67	68	58	46	48	48	44	46	53	57	55	57	47	49
I	70	70	68	73	72	71	87	79	100	83	85	78	81	73	74	73	74	82	77	76	81	65	80	69	66	62	61	56	61	58	35	55	61	45	45	66	69	65	69	43	42
J	72	69	68	73	72	72	83	81	83	100	79	74	75	72	74	73	74	76	74	76	81	67	80	67	64	61	66	62	64	58	46	45	54	47	52	54	56	53	58	47	47
K	73	67	72	77	75	74	85	78	85	79	100	78	85	80	74	75	73	82	79	76	79	66	79	71	74	67	59	55	61	56	41	37	37	50	58	52	58	70	47	47	
Des0	75	72	73	79	77	76	81	75	78	74	78	100	83	79	78	80	84	84	80	79	80	71	77	73	76	69	65	58	63	55	44	59	40	56	56	48	56	56	60	40	48
Des1	84	82	77	85	86	87	82	76	81	75	85	83	100	88	86	88	87	88	85	82	80	73	77	77	78	69	66	61	63	53	37	58	54	52	45	65	56	59	65	56	59
Des2	84	80	77	85	88	87	78	70	73	72	80	79	88	100	88	92	89	83	83	80	76	73	70	82	82	73	73	64	65	51	33	50	59	52	45	72	72	69	69	45	42
CV0	85	85	81	85	88	87	78	73	74	74	74	78	86	88	100	90	92	82	83	86	81	75	81	76	72	78	66	71	51	38	53	69	50	40	59	67	69	63	42	48	
CV1	87	82	84	85	92	90	76	69	73	73	75	80	88	92	90	100	90	82	83	81	76	76	69	83	82	73	73	66	65	51	40	56	62	50	37	70	66	81	55	40	44
CV2	88	83	80	87	89	87	80	72	74	74	73	84	87	89	92	90	100	83	84	83	81	80	73	79	77	73	76	65	71	47	55	30	53	55	55	60	40	60	60	40	65
CV3	78	79	75	83	81	79	86	79	82	76	82	84	88	83	82	82	83	100	84	82	84	71	81	76	77	70	64	60	65	54	31	40	53	40	50	63	68	81	68	50	40

Figure 4. Annotator agreement (all pairs). Left to right: annotator agreement with each other, the learned metric, handcrafted metrics, and VLMs. Annotators background: A-K – 3D modellers. Des0-21 – designers. CV0-31 – computer vision engineers. Best zoom-in.

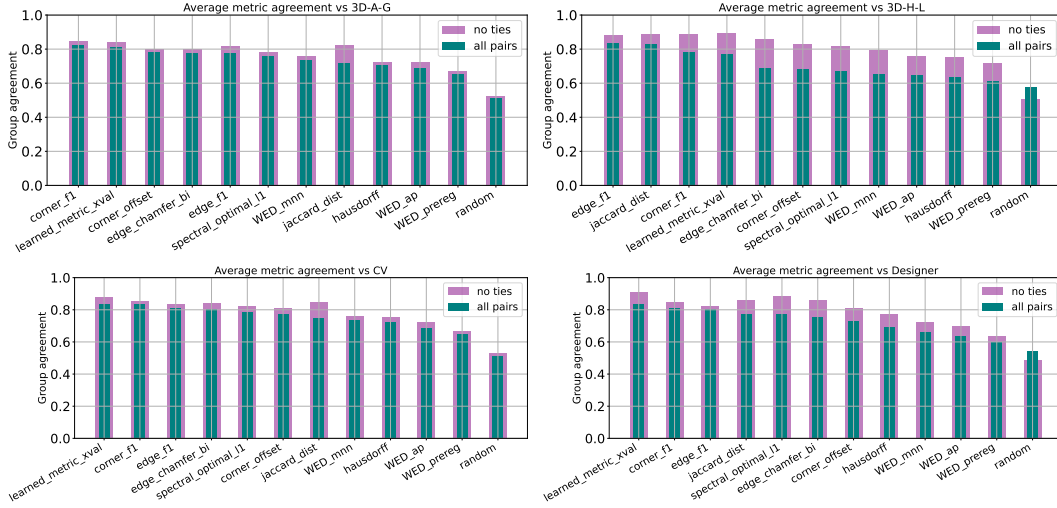


Figure 5. Metric ranking by agreement with group in average. Top: the first group of raters with more attention to vertices, the second group of raters with more attention to edges. Bottom: computer vision engineers, and designers.

consistency score is 89.4%, which could be partially attributed to the labeling mistakes and partially to the changing preferences during the annotation process, which we experienced ourselves.

Finding agreement. We compute an agreement score for each pair for annotators using the following simple rule: the same ranking gets 1 point, the decisive ranking vs "equal" gets 0.5 points, and the opposite ranking gets 0 points.

The agreement table between human annotators, metrics, and VLMs is shown in Fig. 4. The agreement table with all "equal" rankings excluded, is shown in the supplementary.

The average agreement score is around 80% across all annotators, but within clusters, it increases to 85%. When

annotators are decisive (select one of the reconstructions as clearly better rather than selecting "equal"), then the average agreement increases to 90%, and no clusters are observed (see the supplementary). Agreement with the metrics (middle part of Fig. 4) additionally suggests an explanation of cluster preferences.

Observation 4.1

When accounting for ties, there is a moderate, though not strong, global consensus among the human annotators; however, they form two distinct clusters that do not seem to depend on the annotator’s background. One group assigns more weights to the edge accuracy – correlated with edge F1 and Jaccard distance, and the second – vertex accuracy, correlated with corner F1 score.

Cluster 1 (raters A-G, CV, Des1-2) mostly correlates with corner-based metrics, such as corner recall and corner F1-score, whereas Cluster 2 (raters H-K, Des0) correlates more with edge-based metrics, such as edge recall, edge F1-score and Jaccard distance. The second difference between clusters is that Cluster 2 is more likely to give an “equal” score for the low-quality reconstruction, whereas Cluster 1 tried to rank reconstruction more decisively. The metrics ranking w.r.t different groups of raters is shown in Fig. 7. The supplementary material shows the full agreement table.

Observation 4.2

Human annotators pay more attention to correct parts of the reconstruction than the incorrect parts. Regardless of whether edges or vertices are more important, recall metrics agree more with human preferences than precision metrics.

Furthermore, the ranking setup changes the human preferences for different metrics; for example, Jaccard distance performs much better for the decisive pairs compared to all other metrics. WED with pre-registration, which was used in S^23DR challenge, shows the worst correlation and is just slightly better than random chance. Other flavors of the WED metric, namely WED_mnn and WED_AP (used in Building3D Challenge), perform better but still worse than the rest. Graph structure metrics are in the middle. We also consider the agreement with VLMs. Despite initial success with individual examples, we failed to get good results.

Observation 4.3

The average agreement with human preferences of the top handcrafted metrics does not vary significantly. WED-based scores correlate with human judgment the least.

Observation 4.4

VLMs do not show significant agreement with human preferences in the wireframe ranking. The only exceptions are OpenAI models, as well as Grok2. VLMs agree the most with the WED family of the metrics.

Finding the best reconstruction. We explore several ap-

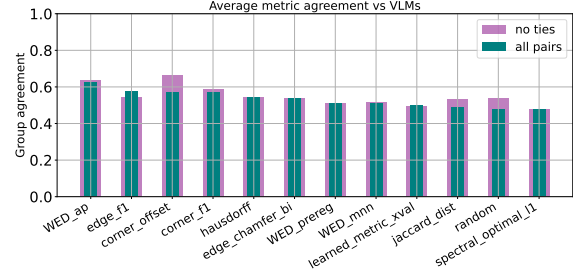


Figure 6. Metric ranking by agreement with VLMs approaches to map these pairwise comparisons to a single “quality” factor. The first approach is similar to chess scoring – first a win-count table is computed. For each rated pair, each method receives 1 point for a win, 0.5 for a tie, and 0 for a loss. This scoring does not break ties but distributes the points evenly. Results with selected reconstruction methods are shown in Fig. 7.

Consistent with the metric-human agreements, recall plays a more important role, and the wireframes with perfect recall – “add_low” and “add_med” are among the leaders in all groups. In other words, extra (erroneous) edges are considered less of an issue when compared to missing an edge or a vertex – the “remove_*” family. One possible explanation resides in the information contained in the reconstruction: if all correct edges are present, we may identify and remove any erroneous ones. However, in many cases, inferring the exact position of an edge or vertex is not possible given the reconstruction alone if key information is missing.

The next set of solutions contains roughly correct but slightly noisy reconstructions - “perturb_*” and “deform_*” family. One of the best solutions from the S23DR Challenge ranked better than highly deformed ground truth but worse than the less invasive corruptions.

The rest of the reconstructions get almost equal scores, which comes from the lots of draws and no wins, among themselves.

Observation 4.5

Human raters tend to rank equally all solutions that are below some quality threshold. Having no solution often ranks slightly better, compared to a totally wrong reconstruction.

We have also modeled the quality of each solution using a Bradley-Terry (BT) [7, 11, 14, 35] preference model on the expressed preferences of the annotators (using the BT-Abilities as scores). The Bradley-Terry model defines the probability that item i is preferred over item j as:

$$P(i > j) = \frac{a_i}{a_i + a_j}, \quad (4)$$

where a_i, a_j are positive real numbers representing the la-

tent strength of each item.

Following standard practice, we reparameterize these latent strengths as exponentials of real-valued parameters θ_i , giving $a_i = e^{\theta_i}$. This yields:

$$P(i > j) = \frac{e^{\theta_i}}{e^{\theta_i} + e^{\theta_j}} = \frac{1}{1 + e^{-(\theta_i - \theta_j)}} = \sigma(\theta_i - \theta_j), \quad (5)$$

where $\sigma(x)$ is the sigmoid function $\sigma(x) = \frac{1}{1 + e^{-x}}$.

This formulation is further generalized by introducing a scale parameter s and offset o :

$$p_{ij} = \sigma\left(\frac{\theta_i - \theta_j}{s} + o\right). \quad (6)$$

With $s = 1$ and $o = 0$, this reduces to the standard Bradley-Terry formulation. Alternatively, setting $s = 400$ and $o = 800$ yields the Elo scoring system familiar to chess players.

To estimate the latent abilities θ , we initialize each θ_i by sampling from an independent Gaussian distribution and then iteratively minimize the expectation of the following binary cross-entropy loss using stochastic gradient descent (SGD) with the Adam optimizer:

$$\mathcal{L} = \mathbb{E}_{(i,j)} [-y \log(p_{ij}) - (1 - y) \log(1 - p_{ij})], \quad (7)$$

where $y = 1$ if item i was chosen over item j , and $y = 0$ otherwise.

To investigate whether the data reflect a single underlying dimension of quality, we additionally peruse a factor analysis based approach. We form the methods-by-raters table M such that M_{kl} is the rate at which rater k chose method l when they saw it. We hypothesize the empirical log-odds of these win-rates (rate l wins according to k), $\eta = \log \frac{M}{1-M}$ possess a low-rank structure (rank one in the ideal case); this would indicate a single dominant factor ("quality") governing outcomes. We apply singular value decomposition (SVD) to factorize $\eta = U\Sigma V^T$ and compute the percent of explained variance as $v_i = \sigma_i^2 / \sum_j \sigma_j^2$ finding $\approx 85\%$ of the variance is explained by the factor corresponding to the largest singular value, while only 5% is explained by the second largest. The left singular vector of η contains the scores. Additionally, we find a Kendall correlation coefficient > 0.93 between the rankings implied by SVD and those implied by BT, lending additional evidence to the hypothesis that there is a true "quality" factor driving the raters' views. The result is shown in Table 1.

Metric properties or "unit tests". For every metric, we design a range of desired properties. Then, we use a dataset of 128 ground truth wireframes, which we disturb or alter and check the behavior of each metric. We report the percentage of wireframes where the property was valid for a given metric. Results are shown in Table 2. Most of the

Method	Empirical Win Rate	Implied Win Rate (BT)	Implied Win Rate (Elo)	BT Ability	Elo Score	Quality Factor
add_low	0.88	0.88	0.89	2.55	1812	-0.35
add_med	0.86	0.87	0.85	2.38	1677	-0.26
add_high	0.83	0.82	0.82	1.88	1533	-0.22
perturb_med	0.82	0.82	0.82	1.92	1560	-0.37
remove_low	0.78	0.77	0.76	1.50	1354	-0.27
perturb_low	0.78	0.77	0.78	1.50	1403	-0.26
deform_med	0.65	0.64	0.65	0.57	1046	-0.15
perturb_high	0.65	0.66	0.66	0.65	1054	-0.13
deform_low	0.64	0.64	0.63	0.53	982	-0.14
remove_high	0.64	0.64	0.65	0.57	1024	-0.10
remove_med	0.63	0.63	0.63	0.50	984	-0.09
kc92	0.51	0.51	0.51	-0.24	683	-0.01
deform_high	0.48	0.48	0.49	-0.43	647	0.00
Siromanec	0.48	0.48	0.49	-0.40	639	-0.00
maximivashechkin	0.39	0.39	0.40	-0.93	432	0.07
rozumden	0.38	0.39	0.37	-0.96	381	0.09
kcml	0.35	0.35	0.36	-1.16	346	0.11
rozumden	0.34	0.33	0.34	-1.28	290	0.11
Ana-Geneva	0.33	0.34	0.32	-1.26	257	0.13
Yurii	0.32	0.32	0.33	-1.38	269	0.13
pc2wf_retrain	0.30	0.30	0.30	-1.48	207	0.15
baseline	0.27	0.27	0.27	-1.66	124	0.22
snuggler	0.27	0.28	0.28	-1.63	143	0.21
Hunter-X	0.24	0.24	0.23	-1.88	32	0.22
TUM	0.24	0.24	0.23	-1.86	22	0.23
Fudan EDLAB	0.23	0.22	0.24	-1.99	41	0.24
pc2wf_pretrained	0.22	0.22	0.21	-2.01	-23	0.26

Table 1. Win rates for selected wireframe, according to the pairwise human annotations and estimated Elo.

metrics pass the triangle inequality test, the identity of indiscernibles, and symmetry. None of the metrics is perfectly monotonic w.r.t. wireframe changes, which makes sense – the precision metrics are insensitive to the number of predicted vertices/edges as long as predicted are correct, etc. Hausdorff and WED with pre-registration pass the worst, which is in line with their poor performance w.r.t. human preferences as well. And the opposite is true – corner F1, edge F1, Jaccard perform well and align with human preferences well. The spectral L1 distance and Chamfer edge distance are exceptions – the spectral distance has scores good on properties, but not human alignment, and Chamfer distance – vice versa.

Additional considerations. After speaking to the human annotators, we note the following. First, the 3D reconstruction experts are considering how the estimated reconstruction could help them in 3D reconstruction. There are two main ways of such help. First is to use the wireframe as a guide to create their own – clean – reconstruction, in case of the noisy reconstruction. The second way, if the reconstruction is already close enough, the wireframe could be fixed to produce the final result. The Wireframe Edit Distance is designed to estimate how costly it would be to fix the predicted wireframe into the correct one. The issue with it is the set of operations – WED only considers vertex/edge deletion/insertion and vertex movement. In practice, one could fit a single edge to multiple noisy ones, bulk-delete a lot of wrong edges or vertices, and apply a rigid transform on the whole reconstruction. All of these operations

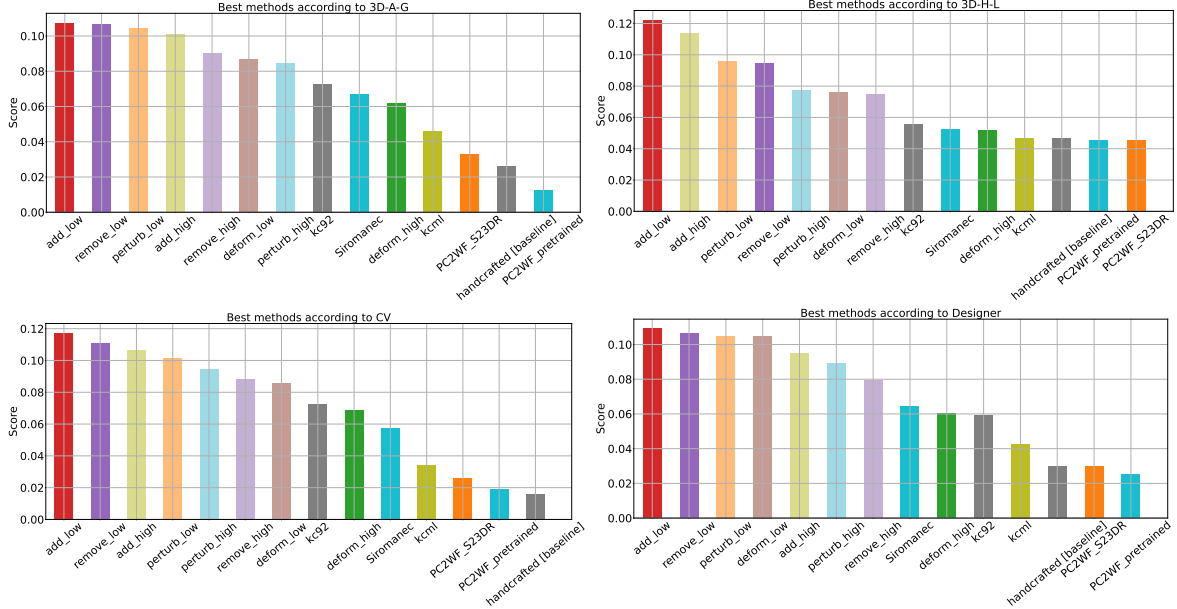


Figure 7. Methods scores according to different groups.

Test	Corner				Edge			WED				Spectral		IoU Jaccard	Hausdorff dist.	Chamfer edge
	Prec	Rec	F1	offset	Prec	Rec	F1	prereg	MNN	nearest	AP	L1	L2			
Monotonic																
Monotonic (wrong edges)	0.02	0.01	0.02	1.00	1.00	0.00	1.00	0.00	0.00	0.00	0.98	0.63	0.14	0.01	0.09	0.00
Monotonic (deform/split)	1.00	0.86	1.00	0.65	1.00	0.98	1.00	0.74	0.79	0.67	0.60	0.00	0.06	0.16	0.05	0.40
Monotonic (moving vertex)	1.00	1.00	1.00	0.98	1.00	1.00	1.00	0.99	1.00	0.99	1.00	0.99	0.99	0.45	0.99	1.00
Monotonic (disconnect edges)	0.52	0.00	0.50	0.31	0.00	0.00	0.00	0.26	1.00	1.00	1.00	0.00	0.01	1.00	0.00	0.02
Monotonic (delete vertices)	0.00	1.00	1.00	1.00	0.00	1.00	1.00	0.75	1.00	1.00	1.00	0.90	0.33	0.67	0.14	0.99
Monotonic (delete edges)	0.00	0.00	0.00	1.00	0.00	1.00	1.00	1.00	1.00	1.00	1.00	1.00	0.31	1.00	0.07	0.83
Identity																
Identity of indiscernibles	1.00	1.00	1.00	1.00	1.00	1.00	1.00	0.02	1.00	1.00	1.0	1.00	1.00	1.00	0.00	0.00
Near identity of indiscernibles	1.00	1.00	1.00	1.00	1.00	1.00	1.00	1.00	1.00	1.00	1.0	1.00	1.00	1.00	0.00	0.00
Symmetry																
Symmetry (0 mean, weighted)	1.00	1.00	1.00	0.88	1.00	1.00	1.00	0.44	0.44	0.44	0.44	0.44	0.90	1.00	0.84	1.00
Near symmetry (0 mean, weighted)	1.00	1.00	1.00	0.87	1.00	1.00	1.00	0.58	0.54	0.54	0.45	0.90	0.92	1.00	1.00	1.00
Symmetry (shift, weighted)	1.00	1.00	1.00	1.00	1.00	1.00	1.00	0.88	0.99	0.92	0.98	0.99	1.00	1.00	0.82	1.00
Near symmetry (shift, weighted)	1.00	1.00	1.00	1.00	1.00	1.00	1.00	1.00	1.00	0.92	0.99	1.00	1.00	1.00	1.00	1.00
Smoothness																
Smoothness (shift, far)	0.00	0.00	0.00	0.00	0.00	0.00	0.00	1.00	0.00	0.00	0.00	1.00	0.72	0.05	0.00	0.00
Smoothness (shift, close)	0.00	0.00	0.00	0.00	0.00	0.00	0.00	1.00	0.16	0.16	0.91	1.00	0.72	0.06	0.00	0.00
Triangle ineq																
Triangle ineq. (rand other)	0.99	1.00	1.00	1.00	1.00	0.98	1.00	1.00	1.00	0.99	0.95	0.92	0.97	1.00	1.00	0.96
Triangle ineq. (add noise)	1.00	1.00	1.00	0.91	1.00	1.00	1.00	0.84	0.81	0.83	1.00	0.90	0.69	1.00	1.00	1.00
Triangle ineq. (del1/del2)	1.00	1.00	1.00	1.00	1.00	1.00	1.00	0.90	0.98	0.98	1.00	1.00	0.66	1.00	1.00	0.43
Pass count																
	11/17	11/17	12/17	11/17	12/17	13/17	14/17	8/17	10/17	10/17	13/17	13/17	8/17	11/17	6/17	8/17

Table 2. Properties "unit-test" results for metrics, percentage of tests passed. The test is passed if the result is $\geq 90\%$ (black).

are commonly used in 3D editing software, and WED could benefit from them.

Finally, if the wireframe is totally wrong, then it is better to have no reconstruction at all and start from scratch. In this "low quality area", most human annotators see no difference between reconstructions, if they both are wrong.

Considering usage in competition and benchmarks, we would recommend to use F1-score, despite the fact that recall-based metrics are more in line with human preferences, as it is less easy to game.

For example, a dense grid of vertices and edges could score perfectly on recall but be useless in practice and score poorly on precision-based metrics.

5. Conclusion

We have studied how human preferences in structured reconstruction evaluation are explained via a wide range of metrics. Human annotators do not have a single preference, and can be split into at least two distinct groups. We show

that human preferences can be learned from a small number of examples by transferring from powerful pretrained models which can subsequently be used to score unseen reconstructions. However, we conclude that additional study is warranted prior to relying on such learned metrics as the sole judging mechanism for competitions (especially those with strong incentives), because of potential for reward hacking, gradient-based adversarial attacks, and the like. Based on our study, we recommend using a combination of edge-based (edge F1 or Jaccard score) and corner-based metrics (F1) for benchmarks and competitions. They better explain human preferences in ranking structured reconstructions than more complex and more fragile graph-based metrics such as WED or spectral distances.

Acknowledgements We thank Sherwin Dale Sotto, Rosalie Cellacay, John Carlo Castro, Johsua Vernon Awog, Romeo Sapitanan, Francis Angel Viloría, Joenard Sarmiento, Danica B. Mercado, Zander Hechanova, Michael James Dulay, Joshua Muñoz, Jonah Franz R. De Leon, Viktor Rusov, Olha Mishkina, Yihe Wang and Tyler Nguyen for their help with wireframe annotations. We also thank Tolga Birdal for helpful discussions at the early stage of the paper.

References

- [1] 1st workshop on urban scene modeling: Where vision meets photogrammetry and graphics. In *Proceedings of the IEEE/CVF Conference on Computer Vision and Pattern Recognition Workshops (CVPRW)*, 2024. 1
- [2] Pravesh Agrawal, Szymon Antoniak, Emma Bou Hanna, Baptiste Bout, Devendra Chaplot, Jessica Chudnovsky, Diogo Costa, Baudouin De Monicault, Saurabh Garg, Theophile Gervet, Soham Ghosh, Amélie Héliou, Paul Jacob, Albert Q. Jiang, Kartik Khandelwal, Timothée Lacroix, Guillaume Lample, Diego Las Casas, Thibaut Lavril, Teven Le Scao, Andy Lo, William Marshall, Louis Martin, Arthur Mensch, Pavankumar Muddireddy, Valera Nemychnikova, Marie Pellat, Patrick Von Platen, Nikhil Raghuraman, Baptiste Rozière, Alexandre Sablayrolles, Lucile Saulnier, Romain Sauvestre, Wendy Shang, Roman Soletskyi, Lawrence Stewart, Pierre Stock, Joachim Studnia, Sandeep Subramanian, Sagar Vaze, Thomas Wang, and Sophia Yang. Pixtral 12b, 2024. 4
- [3] AI Anthropic. Claude 3.5 sonnet model card addendum. *Claude-3.5 Model Card*, 2024. 4
- [4] Andre Araujo, Bingyi Cao, Cam Askew, Jack Sim, Maggie, Tobias Weyand, and Will Cukierski. Google landmark retrieval 2021. <https://kaggle.com/competitions/landmark-retrieval-2021>, 2021. Kaggle. 1
- [5] Armen Avetisyan, Christopher Xie, Henry Howard-Jenkins, Tsun-Yi Yang, Samir Aroudj, Suvam Patra, Fuyang Zhang, Duncan Frost, Luke Holland, Campbell Orme, Jakob Engel, Edward Miller, Richard Newcombe, and Vasileios Balntas. Scenescrypt: Reconstructing scenes with an autoregressive structured language model. In *European Conference on Computer Vision (ECCV)*, 2024. 1
- [6] Eric Brachmann, Jamie Wynn, Shuai Chen, Tommaso Cavallari, Áron Monzspart, Daniyar Turmukhambetov, and Victor Adrian Prisacariu. Scene coordinate reconstruction: Positing of image collections via incremental learning of a relocalizer. In *ECCV*, 2024. 2
- [7] Ralph A. Bradley and Milton E. Terry. Rank analysis of incomplete block designs: I. the method of paired comparisons. *Biometrika*, 39(3/4):324–345, 1952. 4, 6
- [8] Li Cao, Yike Xu, Jianwei Guo, and Xiaoping Liu. Wireframenet: A novel method for wireframe generation from point cloud. *Computers and Graphics*, 115:226–235, 2023. 1
- [9] Jiacheng Chen, Yiming Qian, and Yasutaka Furukawa. Heat: Holistic edge attention transformer for structured reconstruction. In *IEEE Conference on Computer Vision and Pattern Recognition (CVPR)*, 2022. 1
- [10] Kseniya Cherenkova, Elona Dupont, Anis Kacem, Ilya Arzhannikov, Gleb Gusev, and Djamila Aouada. Sepicnet: Sharp edges recovery by parametric inference of curves in 3d shapes. In *2023 IEEE/CVF Conference on Computer Vision and Pattern Recognition Workshops (CVPRW)*, pages 2727–2735, 2023. 2, 3
- [11] Arpad E. Elo. *The Rating of Chessplayers, Past and Present*. Arco Publishing, 1978. Accessed: 2025-03-06. 6
- [12] Gemini Team et al. Gemini: A family of highly capable multimodal models, 2024. 4
- [13] OpenAI et al. Openai o1 system card, 2024. 4
- [14] Mark E Glickman. Introductory note to 1928, 2013. 6
- [15] Tomáš Hodaň, Martin Sundermeyer, Yann Labbé, Van Nguyen Nguyen, Gu Wang, Eric Brachmann, Bertram Drost, Vincent Lepetit, Carsten Rother, and Jiří Matas. BOP challenge 2023 on detection, segmentation and pose estimation of seen and unseen rigid objects. *Conference on Computer Vision and Pattern Recognition Workshops (CVPRW)*, 2024. 1
- [16] Perpetual Hope Akwensi, Akshay Bharadwaj, and Ruisheng Wang. Apc2mesh: Bridging the gap from occluded building façades to full 3d models. *ISPRS Journal of Photogrammetry and Remote Sensing*, 211:438–451, 2024. 2, 3
- [17] Shangfeng Huang, Ruisheng Wang, Bo Guo, and Hongxin Yang. Pbwr: Parametric-building-wireframe reconstruction from aerial lidar point clouds. In *Proceedings of the IEEE/CVF Conference on Computer Vision and Pattern Recognition (CVPR)*, pages 27778–27787, 2024. 2, 3
- [18] Binyuan Hui, Jian Yang, Zeyu Cui, Jiayi Yang, Dayiheng Liu, Lei Zhang, Tianyu Liu, Jiajun Zhang, Bowen Yu, Kai Dang, et al. Qwen2. 5-coder technical report. *arXiv preprint arXiv:2409.12186*, 2024. 4
- [19] Apple Inc. Roomplan: Create 3d floor plans with iphone and ipad. <https://developer.apple.com/augmented-reality/roomplan/>, 2022. 1
- [20] Yuhe Jin, Dmytro Mishkin, Anastasiia Mishchuk, Jiri Matas, Pascal Fua, Kwang Moo Yi, and Eduard Trulls. Image Matching across Wide Baselines: From Paper to Practice. *International Journal of Computer Vision*, 2020. 1, 2

- [21] Matej Kristan, Jiri Matas, Aleš Leonardis, Tomas Vojir, Roman Pflugfelder, Gustavo Fernandez, Georg Nebehay, Fatih Porikli, and Luka Čehovin. A novel performance evaluation methodology for single-target trackers. *IEEE Transactions on Pattern Analysis and Machine Intelligence*, 38(11):2137–2155, 2016. 1
- [22] Jack Langerman, Caner Korkmaz, Hanzhi Chen, Daoyi Gao, Ilke Demir, Dmytro Mishkin, and Tolga Birdal. S23dr competition at 1st workshop on urban scene modeling @ cvpr 2024. <https://huggingface.co/usm3d>, 2024. 1, 2, 3
- [23] L. Leal-Taixé, A. Milan, I. Reid, S. Roth, and K. Schindler. MOTChallenge 2015: Towards a benchmark for multi-target tracking. *arXiv:1504.01942 [cs]*, 2015. arXiv: 1504.01942. 1
- [24] Yujia Liu, Stefano D’Aronco, Konrad Schindler, and Jan Dirk Wegner. Pc2wf: 3d wireframe reconstruction from raw point clouds. In *International Conference on Learning Representations*, 2021. 1, 2, 3
- [25] Yicheng Luo, Jing Ren, Xuefei Zhe, Di Kang, Yajing Xu, Peter Wonka, and Linchao Bao. Lc2wf: learning to construct 3d building wireframes from 3d line clouds. In *Proceedings of the British Machine Vision Conference (BMVC)*, 2022. 1
- [26] Wenchao Ma, Bin Tan, Nan Xue, Tianfu Wu, Xianwei Zheng, and Gui-Song Xia. How-3d: Holistic 3d wireframe perception from a single image. In *International Conference on 3D Vision*, 2022. 1
- [27] Moritz Menze and Andreas Geiger. Object scene flow for autonomous vehicles. In *Conference on Computer Vision and Pattern Recognition (CVPR)*, 2015. 1
- [28] OpenRouter. Openrouter: Unified api for ai models, 2024. Accessed: 2025-03-07. 4
- [29] Maxime Oquab, Timothée Darcet, Theo Moutakanni, Huy V. Vo, Marc Szafraniec, Vasil Khalidov, Pierre Fernandez, Daniel Haziza, Francisco Massa, Alaaeldin El-Nouby, Russell Howes, Po-Yao Huang, Hu Xu, Vasu Sharma, Shang-Wen Li, Wojciech Galuba, Mike Rabbat, Mido Assran, Nicolas Ballas, Gabriel Synnaeve, Ishan Misra, Herve Jegou, Julien Mairal, Patrick Labatut, Armand Joulin, and Piotr Bojanowski. Dinov2: Learning robust visual features without supervision, 2023. 4
- [30] Filip Radenović, Ahmet Iscen, Giorgos Tolias, Yannis Avrithis, and Ondřej Chum. Revisiting oxford and paris: Large-scale image retrieval benchmarking. In *CVPR*, 2018. 1
- [31] Olga Russakovsky, Jia Deng, Hao Su, Jonathan Krause, Sanjeev Satheesh, Sean Ma, Zhiheng Huang, Andrej Karpathy, Aditya Khosla, Michael Bernstein, Alexander C. Berg, and Li Fei-Fei. ImageNet Large Scale Visual Recognition Challenge. *International Journal of Computer Vision (IJCV)*, 115(3):211–252, 2015. 1
- [32] Alberto Sanfeliu and King-Sun Fu. A distance measure between attributed relational graphs for pattern recognition. *IEEE Transactions on Systems, Man, and Cybernetics*, SMC-13(3):353–362, 1983. 3
- [33] Ruisheng Wang, Shangfeng Huang, and Hongxin Yang. Building3D: An Urban-Scale Dataset and Benchmarks for Learning Roof Structures from Point Clouds . In *ICCV*, pages 20019–20029, Los Alamitos, CA, USA, 2023. IEEE Computer Society. 1, 3
- [34] xAI. Grok-2: Advancements in ai language modeling. 2024. Accessed: 2025-03-07. 4
- [35] Ernst Zermelo. Die berechnung der turnier-ergebnisse als ein maximumproblem der wahrscheinlichkeitsrechnung. *Mathematische Zeitschrift*, 29:436–460, 1929. 6
- [36] Yichao Zhou, Haozhi Qi, and Yi Ma. End-to-end wireframe parsing. In *ICCV 2019*, 2019. 1

Explaining Human Preferences via Metrics for Structured 3D Reconstruction

Supplementary Material

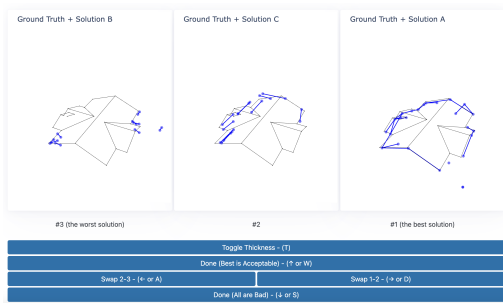


Figure 8. First iteration wireframe ranking interface for human annotators

6. Raking triplets

We have experimented with different forms of ranking the reconstructions, one of which is shown in Figure 8. The annotators were sorting triplets, and also marking if the best solution is acceptable. However, it took people much longer time to process one triplet, and in addition to that, the ranks 2-3 was much less reliable, than 1-2. In the end, we opted for simplicity and also added a message asking annotators to take a break after each 350 pairs.

7. Full agreement tables

The full annotator-metric-VLM agreement table is shown in Figures 10, 11, and the metric rankings are shown in Figure 9.

8. VLM Prompts

All the VLMs are prompted with the following text.

Here we see two possible wireframe reconstructions of houses (shown in blue) superimposed on top of the ground truth wireframe (shown in black). Please describe the quality of each of the two reconstructions (Left and Right). If you don't see any blue lines it is because the reconstruction is incomplete. Which reconstruction most closely matches the ground truth (end by printing the final answer in all caps: "LEFT" or "RIGHT")?

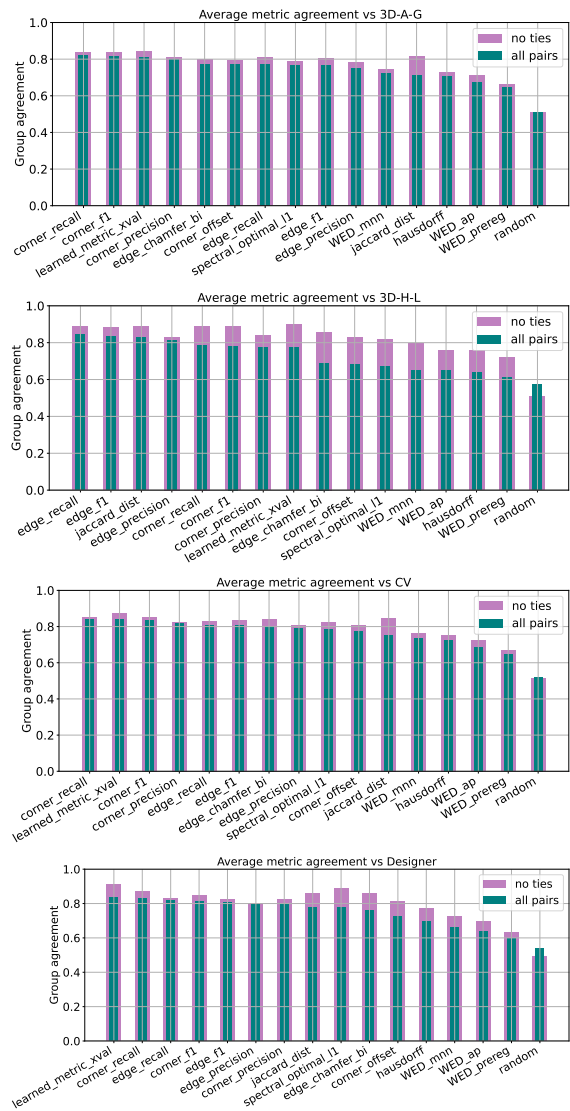


Figure 9. Metric ranking by agreement with group in average. From top to bottom: group of raters 1 with more attention to vertices, group of raters 2 with more attention to edges, computer vision engineers

Annotators agreement, all rankings

	A	B	C	D	E	F	G	H	I	J	K	Des0	Des1	Des2	CV0	CV1	CV2	CV3	learned_metric_xval	corner_f1	corner_offset	edge_f1	jaccard_dist	spectral_optimal_l1	hausdorff	WED_mnn	WED_prereg	WED_ap	random	claude-3.5	claude-3.7	claude-3.7-thinking	gemini-2.0-flash-001	gemini-2.0-flash-lite-001	gpt-4o-2024-11-20	gpt-4o	grok-2-vision-1212	qwen2.5-vl-72b-instruct	pixtral-12b_backup			
A	100	81	79	86	88	87	74	72	70	72	73	75	84	84	85	87	88	78	82	82	78	79	72	77	77	73	73	67	67	50	50	54	52	50	47	52	52	50	54	50	53	
B	81	100	81	83	82	81	73	71	70	69	67	72	82	80	85	82	83	79	77	83	78	80	71	74	71	67	74	65	70	51	50	42	42	54	63	67	67	54	63	45	58	
C	79	81	100	81	84	81	73	67	68	68	72	73	77	77	81	84	80	75	77	77	73	74	68	77	74	65	71	63	67	51	27	41	66	40	31	68	68	68	68	40	40	
D	86	83	81	100	86	85	78	74	73	73	77	79	85	85	85	85	87	83	82	84	81	78	75	77	76	73	72	64	70	51	39	51	55	52	47	58	63	63	64	55	48	
E	88	82	84	86	100	89	76	71	72	72	75	77	86	88	88	92	89	81	83	83	77	78	71	80	77	73	74	66	67	50	43	42	52	45	45	55	62	63	60	50	46	
F	87	81	81	85	89	100	75	70	71	72	74	76	87	87	87	90	87	79	82	82	76	77	71	79	77	71	73	66	67	50	40	50	48	51	47	58	59	58	64	50	46	
G	74	73	73	78	76	75	100	83	87	83	85	81	82	78	78	76	80	86	80	80	85	70	83	71	68	64	68	63	67	56	36	45	56	42	48	58	62	62	67	50	47	
H	72	71	67	74	71	70	83	100	79	81	78	75	76	70	73	69	72	79	74	81	88	70	90	65	61	61	69	67	68	58	46	48	48	44	46	53	57	55	57	47	49	
I	70	70	68	73	72	71	87	79	100	83	85	78	81	73	74	73	74	82	77	76	81	65	80	69	66	62	61	56	61	58	35	55	61	45	45	66	69	65	69	43	42	
J	72	69	68	73	72	72	83	81	83	100	79	74	75	72	74	73	74	76	74	76	81	67	80	67	64	61	66	62	64	58	46	45	54	47	52	54	56	53	58	47	50	
K	73	67	72	77	75	74	85	78	85	79	100	78	85	80	74	75	73	82	79	76	79	66	79	71	74	67	59	55	61	56	41	37	37	50	58	52	58	70	70	47	47	
Des0	75	72	73	79	77	76	81	75	78	74	78	100	83	79	78	80	84	84	80	79	80	71	77	73	76	69	65	58	63	55	44	59	40	56	56	48	56	56	60	40	48	
Des1	84	82	77	85	86	87	82	76	81	75	85	83	100	88	86	88	87	88	85	82	80	73	77	77	78	69	66	61	63	53	37	58	54	52	45	65	56	59	65	56	59	
Des2	84	80	77	85	88	87	78	70	73	72	80	79	88	100	88	92	89	83	83	80	76	73	70	82	82	73	73	64	65	51	33	50	59	52	45	72	72	69	69	45	42	
CV0	85	85	81	85	88	87	78	73	74	74	74	78	86	88	100	90	92	82	83	86	81	81	75	81	76	72	78	66	71	51	38	53	69	50	40	59	67	69	63	42	48	
CV1	87	82	84	85	92	90	76	69	73	73	75	80	88	92	90	100	90	82	83	81	76	76	69	83	82	73	73	66	65	51	40	56	62	50	37	70	66	81	55	40	44	
CV2	88	83	80	87	89	87	80	72	74	74	73	84	87	89	92	90	100	83	84	83	81	80	73	79	77	73	76	65	71	47	55	30	53	55	55	60	40	60	60	40	65	
CV3	78	79	75	83	81	79	86	79	82	76	82	84	88	83	82	82	83	100	84	82	84	71	81	76	77	70	64	60	65	54	31	40	53	40	50	63	68	81	68	50	40	
learned_metric_xval	82	77	77	82	83	82	80	81	76	76	76	79	82	80	86	81	83	82	100	89	85	81	74	70	69	77	69	74	53	34	54	61	51	48	65	66	63	68	46	45		
corner_f1	78	78	73	81	77	76	85	88	81	81	79	80	80	76	81	76	81	84	78	89	100	78	87	71	67	67	75	68	74	55	37	50	63	47	47	67	67	66	72	49	47	
corner_offset	79	80	74	78	77	77	70	70	65	67	66	71	73	73	81	76	80	71	74	85	78	100	70	72	70	67	76	69	72	50	35	57	63	51	50	65	62	61	67	50	45	
jaccard_dist	72	71	68	75	71	71	83	90	80	80	79	77	77	70	75	69	73	81	75	81	87	70	100	67	63	63	68	65	67	57	38	41	46	49	48	55	51	53	60	45	49	
spectral_optimal_l1	77	74	77	77	80	79	71	65	69	67	71	73	77	82	81	83	79	76	78	74	71	72	67	100	77	71	68	61	63	49	31	45	53	43	46	66	63	63	70	47	44	
hausdorff	77	71	74	76	77	77	68	61	66	64	74	76	78	82	76	82	77	77	77	70	67	70	63	77	100	75	61	57	58	50	45	43	45	44	46	48	51	51	57	42	50	
WED_mnn	73	67	65	73	73	71	64	61	62	61	67	69	69	73	72	73	73	70	70	69	67	63	71	75	100	62	55	64	49	51	56	61	47	56	56	51	55	60	50	50	50	
WED_prereg	73	74	71	72	74	73	68	69	61	66	59	65	66	73	78	73	76	64	68	77	75	76	68	68	61	62	100	82	80	49	40	46	49	42	47	55	55	60	62	46	50	
WED_ap	67	65	63	64	66	66	63	67	56	62	55	58	61	64	66	66	65	60	60	69	68	69	65	61	57	55	82	100	67	49	38	47	50	42	47	57	57	62	62	44	51	
random	67	70	67	70	67	67	68	61	64	61	63	63	65	71	65	71	65	64	74	74	72	67	63	58	64	80	67	100	51	38	54	70	44	48	79	75	72	74	51	48		
claude-3.5	50	51	51	51	50	50	56	58	58	58	56	55	53	51	51	51	47	54	54	53	55	50	57	49	50	49	49	51	100	50	50	46	41	42	47	48	49	45	51	47		
claude-3.7	50	50	27	39	43	40	36	46	35	46	41	44	37	33	38	40	55	31	37	34	37	35	38	31	45	51	40	38	38	50	100	47	42	48	55	41	40	41	33	56	62	
claude-3.7-thinking	54	42	41	51	42	50	45	48	55	45	37	59	58	50	53	56	30	40	48	54	50	57	41	45	43	56	46	47	54	50	47	100	73	47	53	58	56	60	60	51	47	
gemini-2.0-flash-001	52	42	66	55	52	48	56	48	61	54	37	40	54	59	69	62	53	53	47	61	63	63	46	53	45	61	49	50	70	46	42	73	100	47	40	68	70	68	73	51	45	
gemini-2.0-flash-lite-001	50	54	40	52	45	51	42	44	45	47	50	56	52	52	50	50	55	40	45	51	47	51	49	43	44	47	42	42	44	41	48	47	47	100	52	48	51	50	52	45	58	
gpt-4o-2024-11-20	47	63	31	47	45	47	48	46	45	52	58	56	45	45	40	37	55	50	50	48	47	50	48	46	46	56	47	47	48	42	55	43	40	52	100	50	48	46	47	55	59	
gpt-4o	52	67	68	63	62	59	62	57	69	56	58	56	56	72	67	66	40	68	55	66	67	62	51	63	51	51	55	57	75	48	40	56	70	51	48	75	100	75	73	74	47	44
o1	50	54	68	63	63	58	62	55	65	53	70	56	59	69	69	81	60	81	52	63	66	61	53	63	51	55	60	62	72	49	41	60	68	50	46	73	76	100	70	47	49	
grok-2-vision-1212	54	63	68	64	60	64	67	57	69	58	70	60	65	69	63	55	60	68	57	68	72	67	60	70	57	60	62	62	74	45	33	60	73	52	47	74	75	70	100	51	46	
qwen2.5-vl-72b-instruct	50	45	40	55	50	50	47	43	47	47	40	56	45	42	40	40	50	51	46	49	50	45	47	42	50	46	44	51	51	56	51	51	45	45	47	42	47	51	100	60	60	
pixtral-12b_backup	53	58	40	48	46	46	47	49	42	50	47	48	59	42	48	44	65	40	45	45	47	45	49	44	50	50	50	51	48	47	62	47	45	58	59	44	40	49	46	60	100	

Figure 10. Annotator-metrics-LLM agreement (all pairs). Annotators background: A-K – 3D modellers, Des[0-2] - designers, CV[0-3] - computer vision engineers. Best zoom-in.

Annotators agreement, no ties

	A	B	C	D	E	F	G	H	I	J	K	Des0	Des1	Des2	CV0	CV1	CV2	CV3	learned_metric_xval	corner_f1	edge_f1	corner_offset	jaccard_dist	spectral_optimal_l1	hausdorff	WED_mnn	WED_prereg	WED_ap	random	claude-3.5	claude-3.7	claude-3.7-thinking	gemini-2.0-flash-001	gemini-2.0-flash-lite-001	gpt-4o-2024-11-20	gpt-4o	grok-2-vision-1212	qwens2.5-vl-72b-instruct	pixtral-12b_backup			
A	100	86	82	94	92	91	94	96	93	94	87	90	93	89	90	91	92	91	86	85	81	81	84	80	81	75	76	69	72	51	50	62	55	51	42	57	57	50	63	52	60	
B	86	100	87	89	86	85	88	94	87	89	78	80	89	87	89	86	85	86	80	87	84	82	82	76	74	69	77	66	74	54	50	37	37	57	71	78	78	57	71	42	64	
C	82	87	100	86	86	83	87	83	86	87	85	89	85	78	82	84	81	86	80	78	77	75	75	78	75	66	72	64	70	52	22	40	70	38	27	72	72	72	72	38	38	
D	94	89	86	100	93	91	91	91	90	92	89	92	92	89	90	91	93	92	86	86	84	83	85	81	81	77	76	67	76	51	34	51	57	53	46	61	69	69	70	58	45	
E	92	86	86	93	100	92	93	91	92	93	89	91	94	91	90	93	91	91	86	85	81	79	82	82	79	74	75	67	71	52	41	39	52	44	44	44	56	65	66	62	51	43
F	91	85	83	91	92	100	93	92	94	94	90	92	95	90	89	92	89	91	85	84	80	78	82	80	78	72	75	67	70	51	36	50	49	52	45	61	63	61	69	50	44	
G	94	88	87	91	93	93	100	89	95	95	89	89	94	90	93	93	95	92	91	89	89	83	87	86	81	75	82	74	78	51	31	44	59	39	48	61	65	65	73	50	43	
H	96	94	83	91	91	92	89	100	86	93	80	82	88	84	94	88	90	83	86	97	96	90	95	82	73	74	92	87	87	49	41	47	47	38	41	58	65	61	67	43	49	
I	93	87	86	90	92	94	95	86	100	94	89	88	96	91	93	94	90	91	87	87	79	87	88	82	75	73	62	69	50	29	57	66	44	44	73	76	70	76	40	39		
J	94	89	87	92	93	94	95	93	94	100	87	88	93	89	93	94	94	90	89	90	88	83	87	84	79	72	83	75	77	51	43	42	57	46	53	57	60	56	64	45	49	
K	87	78	85	89	89	90	89	80	89	87	100	97	95	95	87	94	85	85	89	80	79	76	85	86	92	80	66	58	66	50	36	33	33	50	63	54	63	81	81	45	45	
Des0	90	80	89	92	91	92	89	82	88	88	97	100	91	90	89	94	98	94	90	84	84	82	87	86	91	79	73	62	70	47	42	61	38	57	57	47	57	57	63	36	47	
Des1	93	89	85	92	94	95	94	88	96	93	95	91	100	95	94	96	95	93	91	85	80	79	84	85	86	74	71	64	69	49	28	64	57	54	42	76	61	66	76	61	66	
Des2	89	87	78	89	91	90	90	84	91	89	95	90	95	100	90	95	90	93	86	81	78	75	81	84	84	75	75	65	68	50	33	50	59	52	45	72	72	69	69	45	42	
CV0	90	89	82	90	90	89	93	94	93	93	87	89	94	90	100	91	94	90	86	88	86	83	87	82	77	73	80	68	75	52	38	53	69	50	40	59	67	69	63	42	48	
CV1	91	86	84	91	93	92	93	88	94	94	94	94	96	95	91	100	92	94	87	81	78	77	79	83	82	74	74	66	67	54	40	56	62	50	37	70	66	81	55	40	44	
CV2	92	85	81	93	91	89	95	90	90	94	85	98	95	90	94	92	100	89	87	86	85	82	83	82	79	75	79	67	75	54	56	27	54	56	56	62	37	62	62	37	68	
CV3	91	86	86	92	91	91	92	83	91	90	85	94	93	93	90	94	89	100	89	83	83	80	87	86	88	78	71	64	70	50	30	38	53	40	50	65	70	85	70	50	40	
learned_metric_xval	85	87	78	86	85	84	89	97	87	90	80	84	85	81	88	81	86	83	79	100	92	91	86	77	71	69	79	69	77	52	30	47	62	49	48	73	71	66	75	49	45	
corner_f1	81	84	77	84	81	80	89	96	87	88	79	84	80	78	86	78	85	83	76	92	100	86	88	76	70	70	77	66	77	51	32	45	56	47	49	64	62	64	68	50	48	
edge_f1	81	82	75	83	79	78	83	90	79	83	76	82	79	75	83	77	82	80	74	91	86	100	82	72	70	69	76	69	78	52	33	61	78	48	47	80	80	77	85	51	46	
corner_offset	84	82	75	85	82	82	87	95	87	87	85	87	84	81	87	79	83	87	78	86	88	82	100	78	75	73	73	64	72	52	30	43	50	45	48	66	61	63	70	47	47	
jaccard_dist	80	76	78	81	82	80	86	82	88	84	86	86	85	84	82	83	82	86	79	77	76	72	78	100	77	71	68	61	65	51	31	45	53	43	46	66	63	63	70	47	44	
spectral_optimal_l1	81	74	75	81	79	78	81	73	82	79	92	91	86	84	77	82	79	88	77	71	70	70	75	77	100	75	61	57	60	51	45	43	45	44	46	48	51	51	57	42	50	
hausdorff	75	69	66	77	74	72	75	74	75	72	80	79	74	75	73	74	75	78	70	69	70	69	73	71	75	100	62	55	66	51	51	56	61	47	56	56	51	55	60	50	50	
WED_mnn	76	77	72	76	75	75	82	92	73	83	66	73	71	75	80	74	79	71	70	79	77	76	73	68	61	62	100	82	84	52	40	46	50	42	48	56	56	61	64	47	49	
WED_prereg	69	66	64	67	67	67	74	87	62	75	58	62	64	65	68	66	67	64	65	69	66	69	64	61	57	55	82	100	70	50	35	45	48	41	47	57	57	62	65	45	48	
WED_ap	72	74	70	76	71	70	78	87	69	77	66	70	69	68	75	67	75	70	66	77	77	78	72	65	60	66	84	70	100	51	39	57	72	44	48	80	76	75	77	50	45	
random	51	54	52	51	52	51	51	49	50	51	50	47	49	50	52	54	54	50	51	52	51	52	52	51	51	51	52	50	51	100	51	55	55	55	47	57	52	55	50	51	55	
claude-3.5	50	50	22	34	41	36	31	41	29	43	36	42	28	33	38	40	56	30	40	30	32	33	30	31	45	51	40	35	39	51	100	47	42	48	55	41	40	41	33	56	62	
claude-3.7	62	37	40	51	39	50	44	47	57	42	33	61	64	50	53	56	27	38	43	47	45	61	43	45	43	56	46	45	57	55	47	100	73	47	43	58	56	60	60	51	47	
claude-3.7-thinking	55	37	70	57	52	49	59	47	66	57	33	38	57	59	69	62	54	53	47	62	56	78	50	53	45	61	50	48	72	55	42	73	100	47	40	68	70	68	73	51	45	
gemini-2.0-flash-001	51	57	38	53	44	52	39	38	44	46	50	57	54	52	50	50	56	40	43	49	47	48	45	43	44	47	42	41	44	55	48	47	47	100	52	48	51	50	52	45	58	
gemini-2.0-flash-lite-001	42	71	27	46	44	45	48	41	44	53	63	57	42	45	40	37	56	50	42	48	49	47	48	46	46	46	56	48	47	48	47	55	43	40	52	100	50	48	46	47	55	59
gpt-4o-2024-11-20	57	78	72	61	56	61	61	58	73	57	54	47	76	72	59	70	62	65	52	73	64	80	66	66	48	56	56	57	80	57	41	58	68	48	50	100	75	73	74	47	44	
gpt-4o	57	78	72	69	65	63	65	65	76	60	63	57	61	72	67	66	37	70	57	71	62	80	61	63	51	51	56	57	76	52	40	56	70	51	48	75	100	76	75	42	40	
o1	50	57	72	69	66	61	65	61	70	56	81	57	66	69	69	81	62	85	54	66	64	77	63	63	51	55	61	62	75	55	41	60	68	50	46	73	76	100	70	47	49	
grok-2-vision-1212	63	71	72	70	62	69	73	67	76	64	81	63	76	69	63	55	62	70	58	75	68	85	70	70	57	60	64	65	77	50	33	60	73	52	47	74	75	70	100	51	46	
qwens2.5-vl-72b-instruct	52	42	38	58	51	50	50	43	40	45	45	36	61	45	42	40	37	50	48	49	50	51	47	47	42	50	47	45	50	51	56	51	51	45	55	47	42	47	51	100	60	
pixtral-12b_backup	60	64	38	45	43	44	43	49	39	49	45	47	66	42	48	44	68	40	46	45	48	46																				